Eur. J. Mineral.
2019, **31**, 609–617
Published online 13 April 2019

Crystal-chemical study of ecdemite from Harstigen, a new natural member of the layered lead oxyhalides group

Natale PERCHIAZZI[1,*], Ulf HÅLENIUS[2], Pietro VIGNOLA[3] and Nicola DEMITRI[4]

[1]Dipartimento Di Scienze Della Terra, Università Di Pisa, Via Santa Maria 53, 56126 Pisa, Italy
*Corresponding author, e-mail: natale.perchiazzi@unipi.it
[2]Department of Geosciences, Swedish Museum of Natural History, Box 50007, 0405 Stockholm, Sweden
[3]CNR – Istituto Per La Dinamica Dei Processi Ambientali, Via Botticelli 23, 20131 Milano, Italy
[4]Elettra – Sincrotrone Trieste S.C.P.A., S.S. 14 km 163,5 in Area Science Park – Basovizza, 34149 Trieste, Italy

Abstract: Ecdemite from Harstigen, Värmland, Central Sweden, was studied through Raman and FTIR spectroscopy, electron-microprobe techniques, synchrotron powder and single-crystal diffraction. The ideal mineral formula proposed by Palache, $Pb_6Cl_4As_2O_7$, is confirmed. In contrast to previous suggestions, however, the present study demonstrates that the mineral is monoclinic, with space-group type $P2_1$ and unit-cell parameters a = 10.828(4) Å, b = 10.826(2) Å, c = 6.970(1) Å, β = 113.26°(2). The crystal-structural study of ecdemite shows that the mineral can be considered as made up of regularly alternating Cl layers and litharge-like defective layers, also hosting As cations, with the representative formula $\{Pb_2[Pb_4O](AsO_3)_2\}^{4+}$, in a 1:1 ratio. These features indicate that ecdemite can be considered as a new member of the layered lead oxyhalides group.

Key-words: ecdemite; Harstigen; Sweden; arsenic; lead; layered oxychlorides; FTIR; Raman spectroscopy; synchrotron single-crystal study; synchrotron X-ray powder diffraction pattern.

1. Introduction

Arsenite minerals are quite uncommon in nature, and they are among the most interesting phases of the worldwide famous Långban-type localities in Sweden. Nearly 300 mineral species are known for the group of neighbouring mines at Harstigen, Jakobsberg, Långban, Mangruvan, Nordmark and Sjögruvan, located within ~20 km of each other near the S–E border of the Swedish province of Värmland. Among these, 30 mineral species are unique to these localities and comprise several lead minerals such as oxychlorides (two species), arsenates (four species) and arsenites (eight species).

Among lead arsenites, the crystal structures of freedite (Pertlik, 1987), finnemanite (Effenberger & Pertlik, 1979), gabrielsonite (Perchiazzi *et al.*, 2018), paulmooreite (Araki *et al.*, 1980), trigonite (Pertlik, 1978) were already determined, but the crystal structures of rouseite, heliophyllite and ecdemite have remained unknown.

The present study of ecdemite was performed, together with the crystal-structure study of gabrielsonite (Perchiazzi *et al.*, 2018), within the frame of the SYNTHESYS funded visit SE-TAF-5983 to Naturhistoriska riksmuseet, Stockholm, with the aim of providing further insights into the crystal chemistry of the Pb–As minerals found at the Långban-type deposits.

Nordenskiöld (1877) defined ecdemite as a new species, assigning the mineral to the tetragonal system on the basis of morphological studies, with chemical data pointing to the ideal formula $Pb_7As_2O_8Cl_4$. Moreover, he mentioned the presence of an orthorhombic mineral containing the same elements as ecdemite but not in a sufficient amount to fully define its chemical composition. It was subsequently defined as the new species heliophyllite by Flink (1888). Hamberg (1889) investigated ecdemite or heliophyllite from Harstigen, finding in every sample intergrowths of uniaxial and biaxial lamellae, proposing for them the common formula $Pb_{13}As_4O_{15}Cl_8$. On the basis of Nordenskiöld's (1877) data, Palache *et al.* (1951) proposed the chemical formula $Pb_6Cl_4As_2O_7$ for ecdemite. Sillén & Melander (1941) examined ecdemite and nadorite, $PbSbClO_2$, from Långban as part of their investigations on bismuth oxyhalides with layered structure. They performed X-ray Laue, Weissenberg and precession studies on a cleavage plate of ecdemite from Harstigen. The authors report for ecdemite a *P4/mmm* tetragonal symmetry with a = 10.8, c = 25.6 Å, without any space-group assignment. They commented that "*However plates out of this sample proved under the polarizing microscope to be biaxial.*" Sillén & Melander (1941) performed X-ray powder diffraction and optical studies on ecdemite samples from Jakobsberg and Harstigen. The authors reported that X-ray powder data

https://doi.org/10.1127/ejm/2019/0031-2853 0935-1221/19/0031-2853 $ 4.05

indicate the existence of "*still another phase besides the pseudo-tetragonal one*", also noticing that "*the optical investigation accordingly showed that the crystal plates contain uniaxial parts as well as biaxial ones, the latter with two mutually perpendicular orientations of the axes*." These authors excluded the presence of pentavalent arsenic in ecdemite, but no quantitative chemical data were reported. Welin (1968) in its note on Långban minerals reported X-ray powder diffraction data for ecdemite, indexing the pattern with a tetragonal cell a = 10.8, c = 25.62 Å, without any space-group indication. Jonsson (2003) presented electron-microprobe analyses of ecdemite from Långban and Harstigen, which confirmed the mineral formula proposed by Palache *et al.* (1951). In addition, Jonsson (2003) demonstrated the presence of variable, but significant, concentrations of Sb in many ecdemite samples, which indicated extensive $Sb^{3+} \leftrightarrow As^{3+}$ substitution in ecdemite.

2. Experimental procedures and results

For the present study ecdemite crystals were selected from specimens from the Harstigen Mine, Värmland, Central Sweden, that are preserved in the mineral collections at the Swedish Museum of Natural History in Stockholm under collection numbers NRM19331765 and NRM19331768. Coexisting main phases are rhodonite, calcite and baryte. The ecdemite crystals are translucent with admantine lustre and perfect cleavage. They range in colour from pale greenish yellow to pale yellow and they are optically biaxial negative with $2V \approx 50°$ and the optical X-axis perpendicular to the (001) cleavage plane.

2.1. FTIR spectroscopy

Unpolarized micro-FTIR spectra were recorded on several ground and polished 14 μm thick cleavage fragments of ecdemite crystals from specimen NRM19331765 in the wavenumber range 26.600–5000 cm^{-1} at a resolution of 4 cm^{-1}, using a Bruker Vertex spectrometer equipped with a Hyperion II microscope, a glow-bar source, a KBr beam-splitter and a LN_2-cooled MCT detector.

2.2. Raman spectroscopy

Unpolarized micro-Raman spectra for ecdemite (Fig. 1) were obtained on cleavage plates from both NRM19331765 and NRM19331768 samples, working in back-scattered geometry with a Jobin-Yvon Horiba XploRA Plus apparatus, equipped with a motorized x–y stage and an Olympus BX41 microscope with a 100×/0.75 objective lens. The Raman spectra were excited by a 532 nm emission of a solid-state laser attenuated to 25% intensity, and the system was calibrated using the 520.5 cm^{-1} Raman band of Si before every experimental session. Spectra were collected through repeated multiple acquisition with single counting times of 30 s, and back-scattered radiation was analyzed with a 1200 mm^{-1} grating monochromator.

2.3. Electron-probe microanalysis (EPMA)

Quantitative chemical analyses (Table 1) were performed on polished and carbon coated sections of ecdemite fragments from both NRM19331765 and NRM19331768 samples, each for a total of 10 analysis points, using a JEOL JXA-8200 electron microprobe working in wavelength-dispersion mode, at the laboratory of the Department of Earth Sciences "A. Desio", University of Milan (ESD-MI). The system was operated using an accelerating voltage of 15 kV, a beam current of 5 nA, a spot size of 7 μm, and a counting time for one spot analysis of 30 s on the peaks and 3 s on the right and left backgrounds. The following substances were used as standards: graftonite KF-16 (Fransolet, 1975) for P, Fe, Mn, and Ca; realgar for As; olivine for Mg; hornblende for F; scapolite for Cl; pure metals (99.99 wt%) for Sb and V; synthetic PbO for Pb. Following the structural analysis indications, all the antimony and arsenic are reported as trivalent. Fluorine, P, Ca, V, Mn and Fe were below detection limit in all analyzed points. The raw data were corrected for matrix effects using the ϕρZ method from the JEOL series of programs.

2.4. Single-crystal structural study

Taking advantage of the very good cleavage of ecdemite, a set of 12 progressively smaller cleavage laminas, down to 0.1 × 0.05 × 0.01 mm, were preliminarly investigated by single-crystal intensity-data collection, performed at the Earth Science Department of Pisa University through a Bruker Smart Breeze diffractometer, equipped with an air-cooled CCD detector, with graphite monochromatized Mo $K\alpha$ radiation.

During the indexing procedure of diffraction patterns obtained from the larger crystals, the ecdemite pseudo-tetragonal cell with $a = b \sim 10.8$, $c \sim 25.6$ Å was often proposed by the Bruker ApexIII indexing software. Examination of reciprocal lattice layers from these crystals showed however the presence in the patterns of multiple twinned diffraction domains and constantly of "streaked" reflections along c^*, indicative of structural disorder.

X-ray data obtained on the smallest crystal fragments from specimen NRM19331765 pointed to a monoclinic symmetry for ecdemite, with R_{int} = 0.063 for the reflection dataset. In addition, trials were made to solve the crystal structure of ecdemite in tetragonal and orthorhombic systems. However, the R_{int} values obtained after merging equivalent reflections were quite high: R_{int} = 0.40 for the Laue class *mmm*, and R_{int} = 0.57 for the tetragonal Laue classes 4/*m* and 4/*mmm*.

The preliminary model was subsequently refined through intensity data collected at the XRD1 beamline at the ELETTRA synchrotron facility (Lausi *et al.*, 2015). The ecdemite structure was solved by direct methods with SHELXS-2013 software (Sheldrick, 2013), within the WinGX program suite (Farrugia, 2012). Scattering curves for neutral atoms were taken from the International Tables for Crystallography (Wilson, 1992). Ecdemite is monoclinic with unit-cell parameters a = 10.828(4) Å, b = 10.826(2) Å,

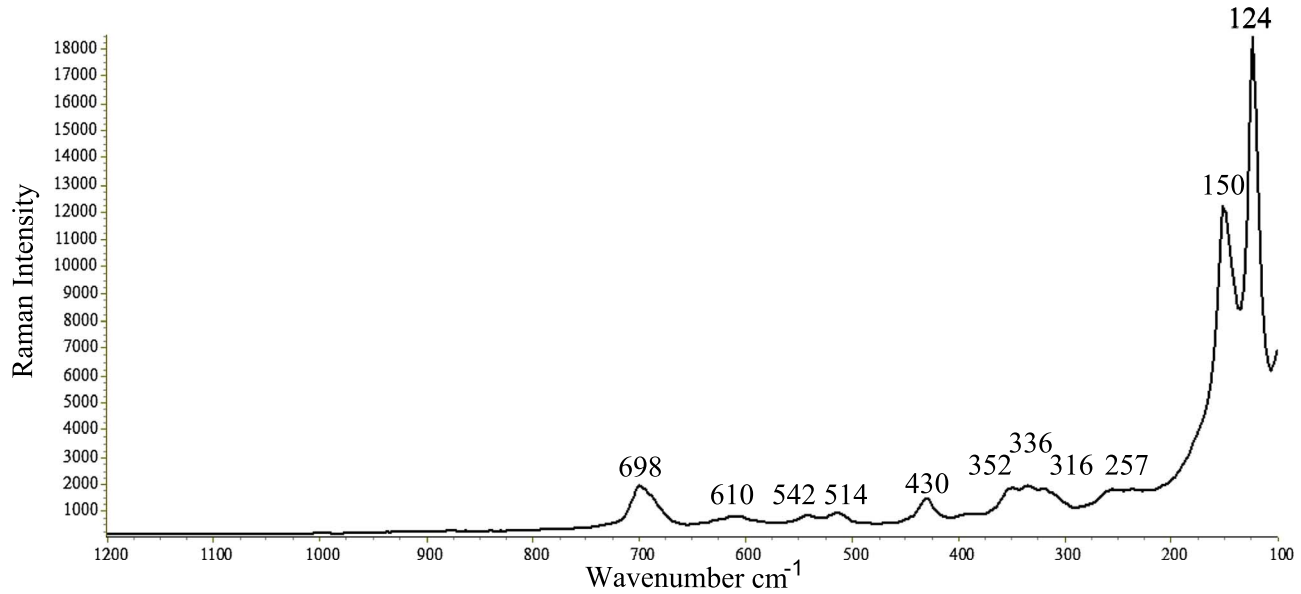

Fig. 1. Raman spectrum of ecdemite sample NRM19331765.

Table 1. Chemical data (in wt%) for ecdemite from Harstigen.

	NRM19331765		NRM19331768	
	n = 10	σ	n = 10	σ
As_2O_3	11.46	0.30	11.71	0.25
Sb_2O_3	0.71	0.13	0.57	0.05
PbO	81.42	0.74	80.73	0.67
Cl	8.66	0.06	9.01	0.11
Σ	102.25		102.01	
–O=Cl	−1.95		−2.20	
Σ	100.30		99.81	

c = 6.970(1) Å, β = 113.26°(2), with space group $P2_1$. The ecdemite pseudo-tetragonal cell can be obtained from the monoclinic true cell through the transformation matrix $\bar{1}00/010/104$. Data pertaining to crystal-structure solution are presented in Table 2. Relatively high residuals in Fourier difference map can be explained with inaccuracies in modelling the anisotropic displacement of Pb atoms, due to the strong absorption of ecdemite, and/or to some degree of structural disorder, highlighted, as reported above, by the presence of streaked reflection along c*.

2.5. Rietveld study

To ascertain the chemical homogeneity of the investigated ecdemite material, some fragments from both NRM19331765 and NRM19331768 samples were ground in acetone, loading the resulting powder into 0.5 mm borosilicate capillaries. Synchrotron X-ray powder diffraction data collections were performed at the XRD1 beamline of the ELETTRA synchrotron facility, and the two collected patterns showed to be almost identical, comparing well also with the ecdemite pattern reported in the Powder Diffraction File database (#23-343). A Rietveld refinement was performed through the TOPAS-Academic program (Coelho, 2018) on the pattern, assuming the ecdemite structure model resulting from the single-crystal study. Nor cell parameters neither the atomic positional and displacement parameters were subsequently refined. A preliminary Pawley refinement (Pawley, 1981) was performed to get starting values for background, modelled with a 1/x function, effective for describing background intensity at low angles due to air scattering, and with a 12-term Chebyshev function. The effect of asymmetry and zero error were accounted for and found to be negligible. The instrumental contribution to the peak shape was modelled through a pseudo-Voigt function, by fitting the data of a sample of SRM 660a (LaB_6) collected under the same experimental setup. Peak-shape broadening was modelled taking into account Gaussian crystallite size and microstrain contributions. The refinement yielded R_{wp} = 3.979, R_{exp} = 1.076, R_p = 3.044, GoF = 3.699, indicating that (Fig. 2) ecdemite is the only phase present in detectable amounts in the analyzed powder.

As it can be seen from Table 3, the X-ray powder pattern agrees quite well with the Welin (1968) data. His dataset, obtained using a Debye-Scherrer geometry and Cu$K\alpha$ radiation, reports the strongest diffractions only, most probably because of the quite strong absorption of ecdemite in this experimental setup. All the diffraction peaks can be satisfactorily indexed with the proposed monoclinic cell.

3. Discussion

Raman studies for lead arsenites occurring at Långban are reported for finnemanite, $Pb_5(AsO_3)_3Cl$, (Bahfenne *et al.*, 2011), paulmooreite, $Pb_2As_2O_5$, (Bahfenne *et al.*, 2012),

Table 2. Experimental details for ecdemite single-crystal structural study.

Crystal data	Data collection and refinement
Crystal-chemical formula	Maximum 2θ; 59.4°
$Pb_6Cl_4As^{3+}_2O_7$	Synchrotron, λ = 0.59041 Å
Crystal size: 0.10 × 0.04 × 0.01 mm	Collected reflections: 47,218
Space group $P2_1$	Unique reflections: 7454, R_{int} = 0.063
a = 10.828(4) Å	Observed reflections: 7410 > 4σ(*Fo*)
b = 10.826(2)	h, k, l $-18 \leq h \leq 18$, $-18 \leq k \leq 18$, $-11 \leq l \leq 11$
c = 6.970(1)	$R[F^2 > 4\sigma(F^2)]$, w$R(F^2)$, S 0.035, 0.092, 1.095
β = 113.26(2)°	Flack x = 0.188(1), $\lvert E^2 - 1\rvert$ = 0.752
V = 750.7(8) Å^3, Z = 2	No. of parameters, restraints: 180, 1
ρ_{calc} = 7.55 g·cm^{-3}, ρ_{meas} = 7.14 g·cm^{-3}	$\Delta\rho_{max}$, $\Delta\rho_{min}$ (e-Å^3) +7.56, −5.77
μ = 7.30 cm^{-1}	

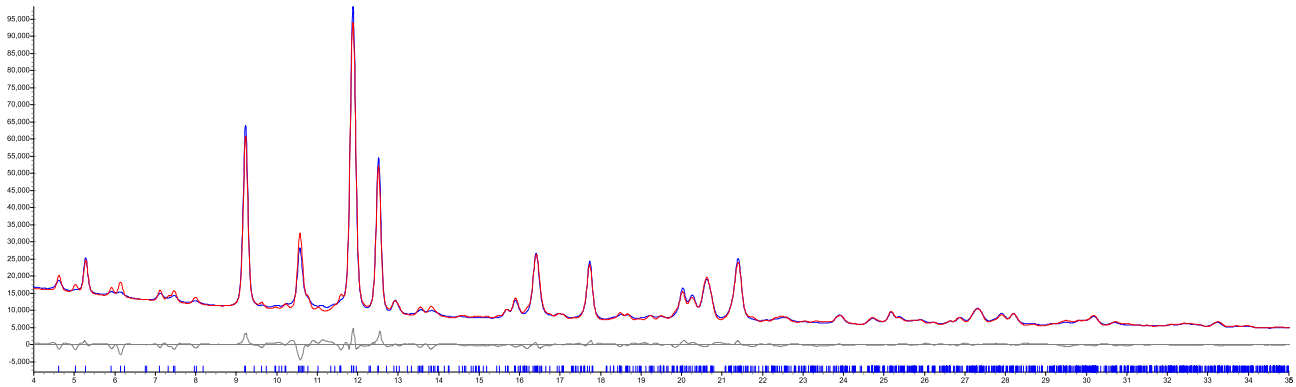

Fig. 2. Final Rietveld refinement plot (2θ°, I = counts) for ecdemite, close-up of the 2θ range 4–35°; red line represents the calculated pattern, blue line the observed pattern. Their difference line is represented as the lower trace, with vertical marks showing the calculated positions for Bragg reflections.

trigonite, $Pb_3Mn^{2+}(AsO_3)_2(HAsO_3)$, (RRUFF database, Lafuente *et al.*, 2015) and gabrielsonite (Perchiazzi *et al.*, 2018). We report in this study the Raman spectrum for ecdemite (Fig. 1). Band assignment can be performed on the basis of the sequence of band energies reported by Nakamoto (1997), namely with $\nu_1 > \nu_3 > \nu_2 > \nu_4$.

In the spectral region 200–1200 cm^{-1} ecdemite shows bands with intensity from medium to weak, due to the symmetric As–O ν_1 (698 cm^{-1}) and antisymmetric ν_3 (610, 542, 514 cm^{-1}) stretching modes, followed at lower wavenumbers by ν_2 (430 cm^{-1}) deformation mode, and in the region centred on 300 cm^{-1} by ν_4 (352, 336, 316, 257 cm^{-1}) deformation mode. Lastly, strong bands due to lattice modes (150 and 124 cm^{-1}) appear in the region below 200 cm^{-1}.

The FTIR spectra in the range 600–5000 cm^{-1} show two absorption bands at 703 and 608 cm^{-1}, which are related to As–O ν_1 and ν_3 stretching modes, respectively. No absorption bands were recorded in the range 750–5000 cm^{-1}, which demonstrates the absence of H_2O, OH^-, BO_3^{3-}, CO_3^{2-} and SO_4^{2-} groups in the crystal structure of ecdemite.

The empirical mineral formulae calculated on the basis of (O + Cl) = 11 apfu for ecdemite from NRM19331765 and NRM19331768 are $Pb_{6.01}As^{3+}_{1.91}Sb^{3+}_{0.08}Cl_{4.02}O_{6.98}$ and $Pb_{5.92}As^{3+}_{1.94}Sb^{3+}_{0.06}Cl_{4.16}O_{6.84}$ respectively. The mineral can be considered as fairly homogeneous, with a minor substitution of As^{3+} with Sb^{3+}, consistent with chemical data reported for ecdemite by Jonsson (2003). An idealized mineral formula is $Pb_6Cl_4As_2O_7$, in agreement with literature data.

Atom positional and displacement parameters, together with bond valence sums, are reported in Table 4. Bond valence sums were calculated according to Krivovichev & Brown (2001) for Pb^{2+}–O bonds and to Brese & O'Keefe (1991) for the remaining bonds. Selected bond lengths (<3.5 Å) for ecdemite are reported in Table 5. During the initial stages of refinement, the two highest peaks in the Fourier difference were localized close to the As1 and As2 sites, possibly indicating a site splitting due to the presence of minor Sb^{3+} substituting for As^{3+}. Positional atomic parameters and a common occupancy by Sb were refined for these two sites, constraining their displacement parameters equal to those of neighbouring As1 and As2 sites. The refined Sb occupancy value is quite close to that measured by EPMA.

The two independent As^{3+} cations occur in the common trigonal pyramidal coordination, with bond distances

Table 3. Synchrotron X-ray powder pattern of NRM19331765 ecdemite (1), compared with Welin (1968) X-ray diffraction pattern (2).

(1)			(2)	
d_{obs} (Å)	*hkl*	I_{obs}	d_{obs} (Å)	I_{obs}
7.328	110	3		
6.409	001	12	6.40	10
5.708	$1\bar{1}\bar{1}$	1		
5.515	011	2		
4.746	120	3		
4.533	210; 111	2		
4.236	111; $12\bar{1}$	1		
3.668	$22\bar{1}$; 220	59	3.66	80
3.386	130	1		
3.300	$11\bar{2}$	2		
3.203	002	20	3.20	30
3.050	012	2	3.05	30
2.852	$2\bar{2}\bar{2}$	100	2.85	100
2.708	$\bar{4}01$; 040	51	2.72	80
2.622	$4\bar{1}\bar{1}$	5	2.64	20
2.499	$13\bar{2}$; $\bar{4}02$	2		
2.451	122	2		
2.335	141	<1		
2.233	$1\bar{1}\bar{1}$	<1	2.22	10
2.163	$4\bar{3}\bar{1}$; $3\bar{4}\bar{1}$	3		
2.135	003; $14\bar{2}$	6	2.13	10
2.069	042	21	2.07	70
2.001	$5\bar{2}\bar{1}$	2		
1.915	$4\bar{4}\bar{1}$	19	1.92	60
1.836	$5\bar{3}\bar{1}$	2		
1.820	$5\bar{3}\bar{2}$; 251	2		
1.768	$5\bar{2}\bar{3}$	2		
1.697	511; 260; $6\bar{2}\bar{1}$	11		
1.678	043	9	1.670	40
1.649	223; $6\bar{1}\bar{3}$	14	1.652	50
1.590	$2\bar{6}\bar{2}$; 261	21	1.591	70
1.509	162; $1\bar{7}\bar{1}$; 630	2		
1.426		3	1.428	20
1.379		2		
1.354		4		
1.343		3		
1.317		2		
1.281		1		
1.270		2		
1.250		5	1.253	30
1.224		4		
1.212		4		
1.193		1		
1.171		1		
1.160		1		
1.146		2		
1.134		3		
1.115		1		
1.032		2		
1.009		<1		

Table 4. Fractional atomic coordinates, equivalent isotropic displacement parameters (Å^2) and bond valence sums for ecdemite. A common occupancy for As1 and As2 sites was refined to As 0.924(3), together with a common occupancy for split Sb1 and Sb2 sites of Sb 0.076(3).

Atom	BVS	*x*	*y*	*z*	*U*eq
Pb1	2.08	0.57617(5)	−0.59182(4)	−0.23268(7)	0.01374(8)
Pb2	1.99	0.69599(5)	−0.83328(4)	0.21134(8)	0.01470(9)
Pb3	1.99	0.80428(5)	−0.34997(4)	0.73947(8)	0.01499(9)
Pb4	1.96	−0.08096(6)	−0.11308(4)	−0.77878(9)	0.0172(1)
Pb5	1.92	0.84231(5)	−0.86357(5)	−0.19313(8)	0.01529(9)
Pb6	1.90	0.43812(5)	−0.58290(5)	0.19625(8)	0.01508(9)
As1	2.72	0.6390(1)	−0.3252(1)	0.1510(2)	0.0098(2)
Sb1	0.19	0.331(1)	0.142(1)	0.788(2)	0.0098(2)
As2	2.64	0.062(1)	−0.1168(1)	−0.1478(3)	0.0101(2)
Sb2	0.19	0.065(1)	0.908(1)	0.796(2)	0.0101(2)
Cl1	0.91	0.0029(3)	−0.3619(4)	−0.4629(6)	0.0211(6)
Cl2	0.99	0.7612(4)	−0.6057(4)	0.4916(7)	0.0251(7)
Cl3	0.88	0.4685(3)	−0.3339(3)	0.4613(6)	0.0198(5)
Cl4	0.76	0.7354(4)	−0.0907(4)	0.4941(6)	0.0225(6)
O1	1.98	0.537(1)	−0.4506(9)	0.002(2)	0.018(2)
O2	1.96	0.776(1)	−0.6871(9)	0.002(2)	0.017(2)
O3	1.89	0.722(1)	−0.269(1)	−0.005(2)	0.021(2)
O4	2.10	0.503(1)	−0.2141(9)	0.041(2)	0.015(2)
O5	1.88	0.757(1)	−0.9769(9)	0.006(2)	0.015(2)
O6	2.06	−0.025(1)	−0.225(1)	−0.047(2)	0.018(2)
O7	1.92	0.951(1)	−0.495(1)	0.982(2)	0.021(2)

Table 5. Selected bond distances (Å) for ecdemite. Bond lengths <3.5 Å were taken into account for Pb coordination.

Pb1		Pb2		Pb3		As1	
–O4	2.27(1)	–O5	2.38(1)	–O6	2.303(9)	–O3	1.77(1)
–O2	2.37(1)	–O4	2.529(9)	–O7	2.40(1)	–O1	1.80(1)
–O1	2.39(1)	–O2	2.53(1)	–O3	2.44(1)	–O4	1.82(1)
–Cl3	3.005(4)	–O1	2.69(1)	–Cl1	3.005(5)		
–Cl4	3.138(4)	–Cl1	3.047(3)	–Cl2	3.198(4)	Sb1	
–Cl2	3.282(6)	–Cl2	3.049(4)	–Cl4	3.218(4)	–O1	1.88(1)
–Cl3	3.427(4)	–Cl4	3.342(4)	–Cl3	3.382(3)	–O3	2.05(2)
		–Cl3	3.404(4)			–O4	2.32(1)
Pb4		Pb5		Pb6		As2	
–O5	2.332(9)	–O5	2.30(1)	–O5	2.323(9)	–O7	1.80(1)
–O6	2.50(1)	–O6	2.52(1)	–O4	2.45(1)	–O2	1.810(9)
–O7	2.67(1)	–O7	2.57(1)	–O1	2.49(1)	–O6	1.81(1)
–O3	2.69(1)	–O2	2.60(1)	–O3	2.65(1)		
–Cl1	3.134(4)	–Cl3	3.155(3)	–Cl3	3.211(4)	Sb2	
–Cl2	3.244(4)	–Cl4	3.185(4)	–Cl2	3.294(4)	–O7	1.93(2)
–Cl4	3.259(5)	–Cl1	3.425(4)	–Cl4	3.376(5)	–O2	2.03(1)
–Cl1	3.369(4)	–Cl2	3.445(4)	–Cl3	3.492(4)	–O6	2.25(2)

showing a quite limited variation, clustering near a mean value of 1.801 Å, close to the mean value of 1.782 Å for As–(O, OH) distances reported by Majzlan *et al.* (2014).

The coordination environments of the six independent Pb atoms in the ecdemite structure are shown in Fig. 3. All Pb atoms are linked to four Cl, in the bond range 3.00–3.49 Å, and to three or four oxygens, in the range 2.27–2.69 Å. The Pb1 and Pb3 atoms are seven-coordinated; Pb2, Pb4, Pb5 and Pb6 atoms are eight-coordinated in a distorted square antiprism configuration.

All six-coordination environments have highly asymmetric dispositions of anions, with the oxygen and chlorine atoms located on opposite sides with respect to the Pb cations. This disposition of anions is frequently found in lead oxyhalides (Krivovichev & Brown, 2001; Krivovichev

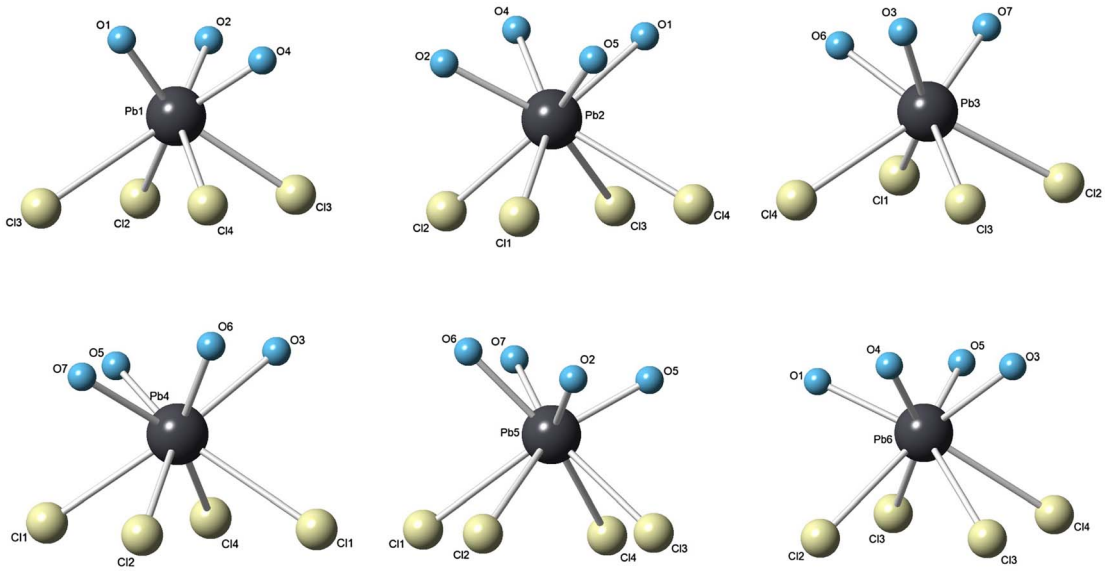

Fig. 3. Coordination polyhedra of the six independent Pb atoms (black colour) in ecdemite structure. Oxygen and chlorine atoms are represented in cyan and light yellow, respectively.

& Burns, 2001, 2002; Siidra *et al.*, 2007, 2013a and b) and according to these authors is consistent with the presence of an active "lone pair" effect of Pb^{2+}, with the $6s^2$ inert electron doublet ideally located towards the plane hosting the Cl anions.

Chlorine coordination range from IV for Cl1, to VI for Cl2 and Cl4 and lastly to VII for Cl3. Oxygen anions are in a slightly distorted tetrahedral coordination, made up by three Pb and one (As, Sb) atoms, with the exception of O5, which is tetrahedrally coordinated by four lead atoms.

4. Structure description and relationships to the layered lead oxyhalides structural group

The crystal structure of ecdemite (Fig. 4) is closely related to the group of lead oxyhalides referred as Aurivillius phases (Aurivillius, 1982, 1983). These crystal structures can be conveniently described through litharge derivative layers, made up by oxocentered OPb_4 tetrahedra (Boher *et al.*, 1985), regularly alternating with layers of Cl anions. Removing OPb_4 tetrahedra from the ideal litharge layers leads to the formation of derivative litharge layers with variable stoichiometry $[Pb_mO_n]^{z+}$, with $m > n$, and charge balance maintained by Cl layers. Stacking sequences with a 1:1 and 2:1 litharge/chlorine layers ratio are found in synthetic and natural phases (Krivovichev *et al.*, 2009, 2013). The weaker Pb–Cl bonds account for the perfect cleavage showed by all these structurally related phases.

The crystal structure of a large number of naturally occurring lead oxychlorides can be built with these structural modules (Krivovichev & Filatov, 1999; Siidra *et al.*, 2008a and b, 2011, 2013a and b; Turner *et al.*, 2012) as well as in synthetic oxyhalides (Siidra *et al.*, 2013c, 2016).

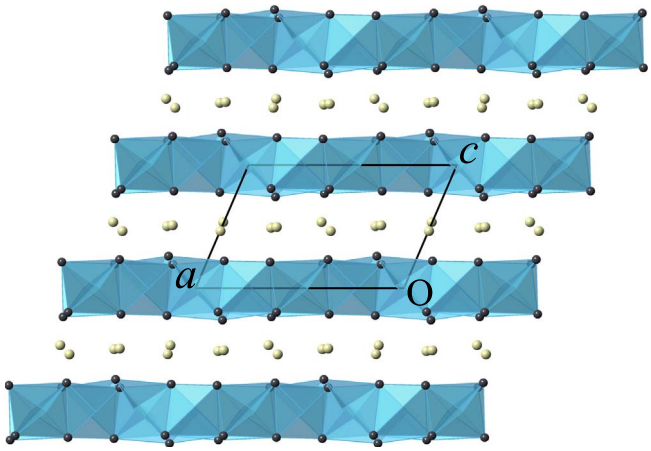

Fig. 4. Crystal structure of ecdemite as seen along [010]. Layers formed by edge-sharing oxocentred OPb_4 (cyan) regularly alternate with layers hosting Cl atoms (yellow).

In rumseyite (Turner *et al.*, 2012), fully occupied oxocentered litharge layers host the $O^{2-} \leftrightarrow F^-$ substitution, with charge balance maintained by the insertion of chlorine layers. A related structure, with fully occupied layers of fluocentered FPb_4 tetrahedra is found in matlockite (Pasero & Perchiazzi, 1996), showing a 1:2 sequence of FPb_4:Cl:Cl layers. Triangular or tetrahedral structural units can be inserted in the voids left by vacant OPb_4 tetrahedra in litharge derivative layers (Fig. 5a). Tetrahedral groups can be represented by SO_4, as in symesite structure (Welch *et al.*, 2000), AsO_4 (sahlinite, Bonaccorsi & Pasero, 2003), SiO_4 (asisite, Welch, 2004), VO_4 (kombatite, Cooper & Hawthorne, 1994). In blixite (Krivovichev & Burns, 2006) and mereheadite (Krivovichev *et al.*, 2009) hydroxyl

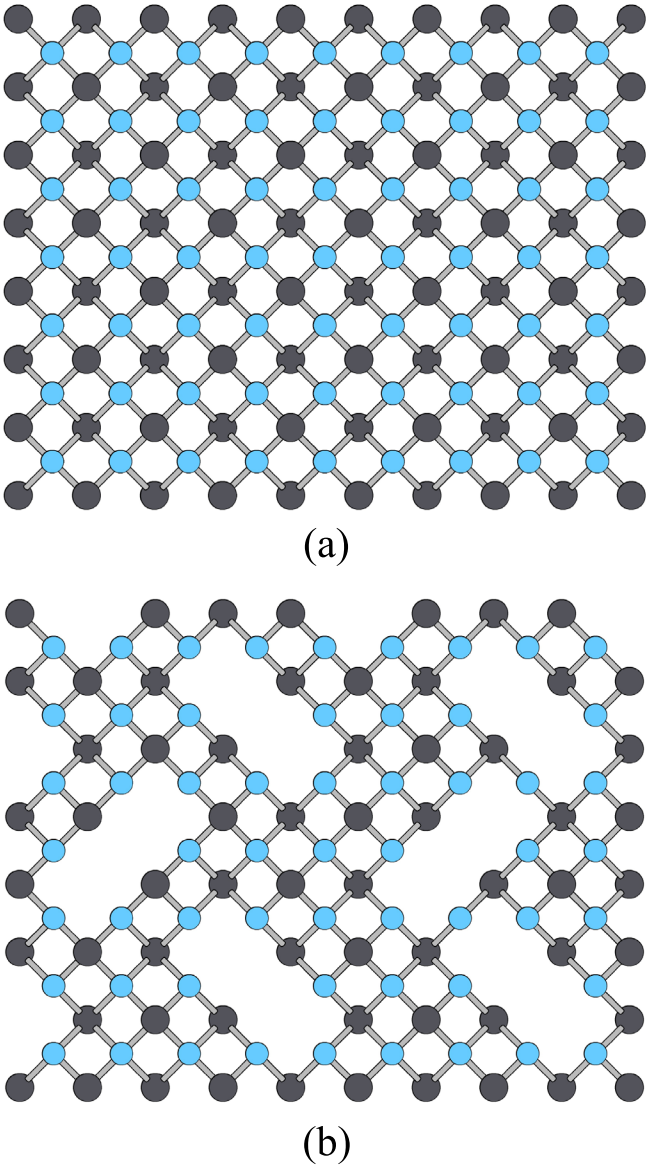

Fig. 5. (a) Ball-and-stick comparison of the fully occupied PbO layer in litharge and (b) partially vacant PbO layer in ecdemite. Oxygen and lead atoms are represented as cyan and black spheres, respectively.

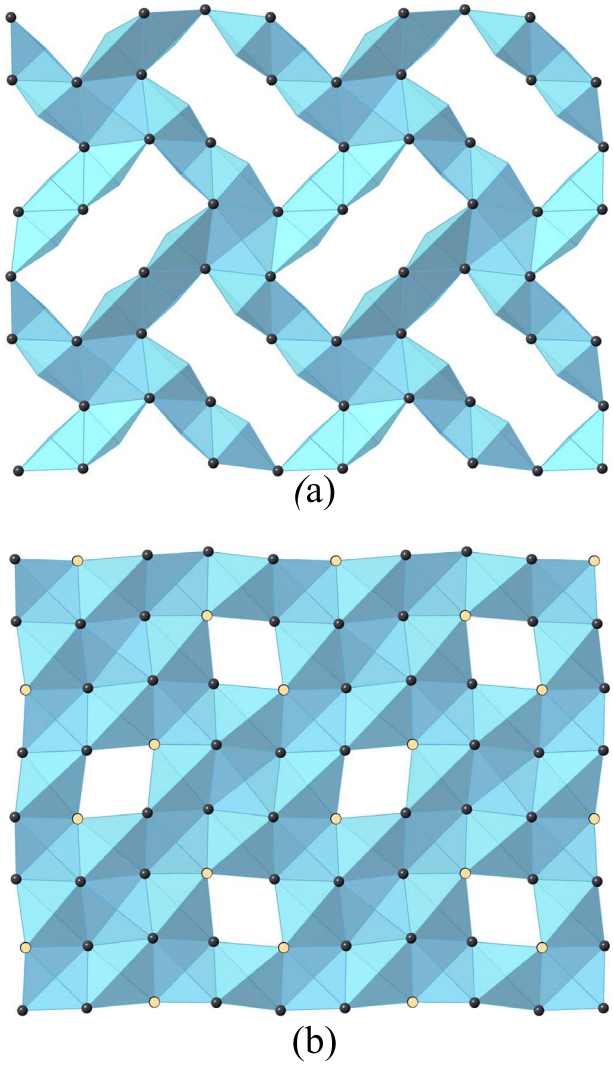

Fig. 6. Comparison of litharge-like layers in ecdemite: (a) polyhedral oxocentred OPb_4 representation of vacant PbO layer in ecdemite; (b) litharge-like layers represented as heterometallic oxocentred OPb_3As tetrahedra. Lead and arsenic atoms are represented as black and light orange spheres, respectively.

groups are linked as $(OH)Pb_2$ dimers to the litharge derivative layers, substituting for vacant O^{2-} in the layers. Triangular CO_3 and BO_3 groups are moreover found in mereheadite (Krivovichev *et al.*, 2009).

In ecdemite (Fig. 5b), two Pb and one oxygen atom positions are left vacant in the litharge-like layers, leading to a layer formula $[Pb_6O_7]^{2-}$, hosting rectangular-shaped voids in which two $^{III}As^{3+}$ cations are inserted (Fig. 6a). The layer voids are appropriate sites for hosting electron lone pairs of both As and Pb atoms. Alternatively, one should consider the occurrence of edge-sharing heterometallic oxocentred tetrahedra OPb_3As, forming heterometallic layers with formula $(Pb_6As_2O_7)^{4+}$ (Fig. 6b), in which 1/8 of the oxygen positions remains vacant, the charge balance being maintained by the insertion of Cl layers (Fig. 7a) with a 1:1 stacking sequence.

It should be noticed, however, that only O5 forms homometallic oxocentered OPb_4 tetrahedra, being bonded to Pb2, Pb4, Pb5, Pb6 atoms (Fig.7b), with the remaining oxygen atoms forming additional strong bonds with (As, Sb) atoms. Homometallic ($O5Pb_4$) tetrahedra are isolated within the heterometallic layers (Fig. 7b), with the two remaining independent lead atoms, Pb1 and Pb3, linked to oxygen atoms belonging to $[(As,Sb)O_3)]$ groups. The crystal-chemical formula representative of heterometallic layers should therefore more properly be written as $\{Pb_2[Pb_4O](AsO_3)_2\}^{4+}$, leading to the crystal-chemical formula $Pb_2[Pb_4O](AsO_3)_2Cl_4$ for ecdemite.

Whereas the Cl layer (Fig. 7a) shows a neat pseudotetragonal symmetry, the true non-centrosymmetric nature of

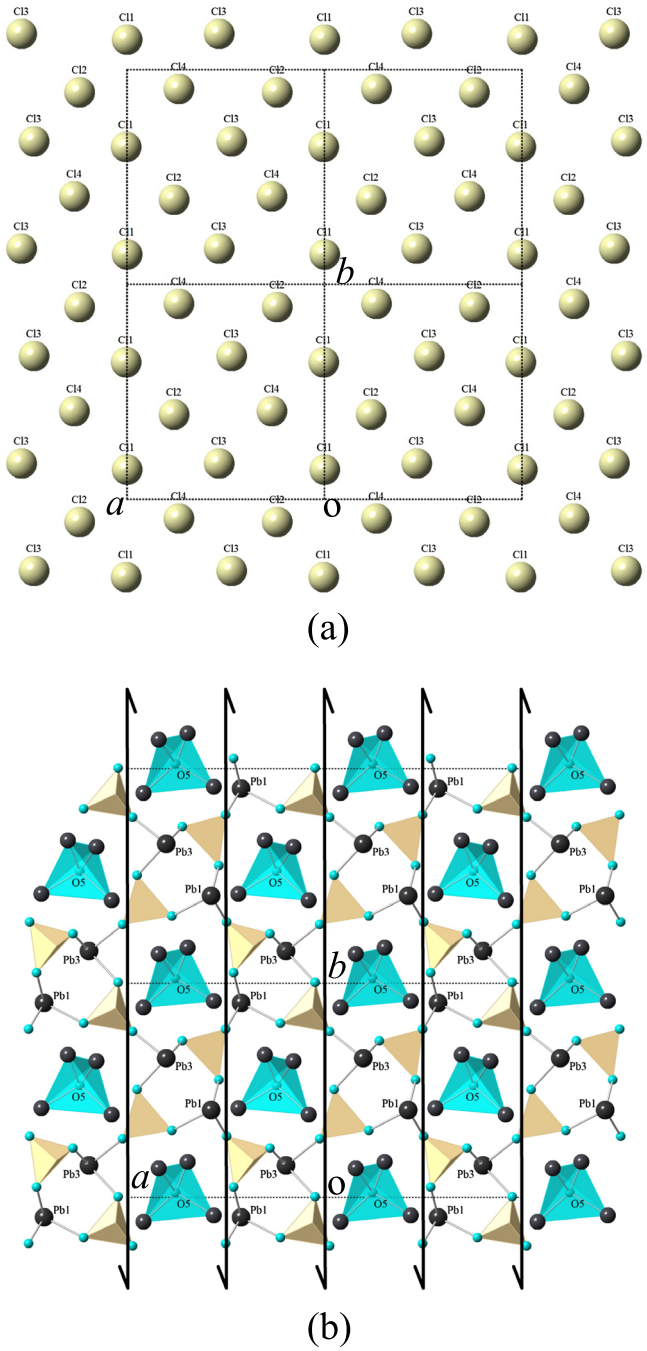

Fig. 7. Comparison of the Cl layer (a) and of the heterometallic layer (b) with representative crystal-chemical formula $\{Pb_2[Pb_4O](AsO_3)_2\}^{4+}$, in ecdemite. Pb2, Pb4, Pb5, Pb6 atoms coordinate O5 oxygen atoms forming isolated homometallic (OPb_4) tetrahedra. Interlayer bonding of Pb1 and Pb3 atoms is moreover reported, together with (As,Sb) trigonal pyramids. The Cl layer shows a clear pseudo-tetragonal symmetry, whereas the true acentric symmetry of ecdemite is evident from the atom arrangement in the heterometallic layer. Oxygen and lead atoms are represented as cyan and black spheres respectively, arsenic as light orange trigonal pyramids.

ecdemite can be better viewed in Fig. 7b, which highlights the $\{Pb_2[Pb_4O](AsO_3)_2\}^{4+}$ heterometallic layers and clearly demonstrates the presence of a two-fold screw axis (2_1) in the ecdemite structure.

5. Conclusions

A crystal-chemical study of ecdemite from the Långban-type deposit at Harstigen,Värmland, Central Sweden confirms the ideal mineral formula, $Pb_6Cl_4As_2O_7$, suggested by Palache *et al.* (1951). The single-crystal structure study demonstrates that the mineral is monoclinic, $P2_1$, a = 10.828(4) Å, b = 10.826(2) Å, c = 6.970 (1) Å, β = 113.26°(2). The mineral belongs to the group of layered Pb oxychlorides, and its crystal structure can be described by a 1:1 succession of Cl layers regularly alternating with defective PbO layers, hosting As^{3+} in the layer voids, with the formula $\{Pb_2[Pb_4O](AsO_3)_2\}^{4+}$ – yielding the crystal-chemical formula $Pb_2[Pb_4O](AsO_3)_2Cl_4$.

Acknowledgements: This research received support from the SYNTHESYS Project (http://www.synthesys.info/), which was financed by European Community Research Infrastructure Action under the FP7 "Structuring the European Research Area Programme". This work was financially supported by the University of Pisa through the project PRA_2018_41 "Georisorse e Ambiente". The authors wish to thank A. Pavese, University of Turin, for providing funds for the EPMA analyses**.** Constructive comments on this manuscript by Oleg Siidra and an anonymous reviewer are greatly appreciated.

References

Araki, T., Moore, P.B., Brunton, G.D. (1980): The crystal structure of paulmooreite, $Pb_2[As_2O_5]$: dimeric arsenite groups. *Am. Mineral.*, **65**, 340–345.

Aurivillius, B. (1982): On the crystal-structure of a number of nonstoichiometric mixed lead-oxide halides composed of PbO like blocks and single halogen layers. *Chem. Scr.*, **19**, 97–107.

— (1983): On the crystal structure of some non-stoichiometric mixed lead oxide halides and their relation to the minerals "lorettoite" and sundiusite. *Chem. Scr.*, **22**, 5–11.

Bahfenne, S., Rintoul, L., Langhof, J., Frost, R.L. (2011): Single-crystal Raman spectroscopy of natural finnemanite and comparison with its synthesised analogue. *J. Raman Spectr.*, **42**, 2119–2125.

—, —, —, — (2012): Single-crystal Raman spectroscopy of natural paulmooreite $Pb_2As_2O_5$ in comparison with the synthesized analog. *Am. Mineral.*, **97**, 143–149.

Boher, P., Garnier, P., Gavarri, J.R., Hewat, A.W. (1985): Monoxyde quadratique PbOα (I): Description de la transition structurale ferroélastique. *J. Solid State Chem.*, **57**, 343–350.

Bonaccorsi, E. & Pasero, M. (2003): Crystal structure refinement of sahlinite, $Pb_{14}(AsO_4)_2O_9Cl_4$. *Mineral. Mag.*, **67**, 15–21.

Brese, N.E. & O'Keeffe, M. (1991): Bond-valence parameters for solids. *Acta Crystallogr.*, **B47**, 192–197.

Coelho, A.A. (2018): TOPAS and TOPAS-Academic: an optimization program integrating computer algebra and crystallographic objects written in C++. *J. Appl. Crystallogr.*, **51**, 210–218.

Cooper, M. & Hawthorne, F.C. (1994): The crystal structure of kombatite, $Pb_{14}(VO_4)_2O_9Cl_4$, a complex heteropolyhedral sheet mineral. *Am. Mineral.*, **79**, 550–554.

Effenberger, H. & Pertlik, F. (1979): The crystal structure of finnemanite, $Pb_5Cl(AsO_3)_3$, with a comparison to the structure-type of chlorapatite, $Ca_5Cl(PO_4)_3$. *Mineral. Petrol.*, **26**, 95–107.

Farrugia, L.J. (2012): WinGX and ORTEP for Windows: an update. *J. Appl. Crystallogr.*, **45**, 849–854.

Flink, G. (1888): Heliophyllit von Pajsberg. *Öfvers. Kongl. Vetensk.-Akad. Förh.*, **45**, 574–578.

Fransolet, A.M. (1975): Etude minéralogique et pétrologique des phosphates de pegmatites granitiques. Unpublished PhD Thesis, University of Liège, Liège, Belgium, 333 p.

Hamberg, A. (1889): Optische Anomalien des Ekdemit (Heliophyllit) von Harstigen. *Geol. Fören. Förh.*, **11**, 229–237.

Jonsson, E. (2003): Mineralogy and parageneses of Pb oxychlorides in Långban-type deposits, Bergslagen, Sweden. *Geol. Fören. Förh.*, **125**, 87–98.

Krivovichev, S.V. & Brown, I.D. (2001): Are the compressive effects of encapsulation an artifact of the bond valence parameters? *Z. Krist.*, **216**, 245–247.

Krivovichev, S.V. & Burns, P.C. (2001): Crystal chemistry of lead oxide chlorides. I. Crystal structures of synthetic mendipite, $Pb_3O_2Cl_2$, and synthetic damaraite, $Pb_3O_2(OH)Cl$. *Eur. J. Mineral.*, **13**, 801–809.

—, — (2002): Crystal chemistry of lead oxide chlorides. II. Crystal structure of $Pb_7O_4(OH)_4Cl_2$. *Eur. J. Mineral.*, **14**, 135–139.

—, — (2006): The crystal structure of $Pb_8O_5(OH)_2Cl_4$, a synthetic analogue of blixite? *Can. Min.*, **44**, 515–522.

Krivovichev, S.V. & Filatov, S.K. (1999): Structural principles for minerals and inorganic compounds containing anion-centered tetrahedra. *Am. Mineral.*, **84**, 1099–1106.

Krivovichev, S.V., Turner, R., Rumsey, M., Siidra, O.I., Kirk, C.A. (2009): The crystal structure and chemistry of mereheadite. *Mineral. Mag.*, **73**, 103–117.

Krivovichev, S.V., Mentre, O., Siidra, O.I., Colmont, M., Filatov, S.K. (2013): Anion-centered tetrahedra in inorganic compounds. *Chem. Rev.,* **113**, 6459–6535.

Lafuente, B., Downs, R.T., Yang, H., Stone, N. (2015): Highlights in mineralogical crystallography. W. De Gruyter, Berlin, 1–30.

Lausi, A., Polentarutti, M., Onesti, S., Plaisier, J.R., Busetto, E., Bais, G., Pifferi, A. (2015): Status of the crystallography beamlines at Elettra. *Eur. Phys. J. Plus*, **130**, 43.

Majzlan, J., Drahota, P. & Filippi, M. (2014): Parageneses and crystal chemistry of arsenic minerals. *Rev. Mineral. Geochem.*, **79**, 17–184.

Nakamoto, K. (1997): Infrared and Raman spectra of inorganic and coordination compounds. Part A: Theory and applications in inorganic chemistry. 5th ed. Wiley-Interscience, New York.

Nordenskiöld, A.E. (1877): Nya mineralier från Långban. *Geol. Fören. Förh.*, **3**, 376–384.

Palache, C., Berman, H., Frondel, C., Dana, E.S. (1951): The system of mineralogy of James Dwight Dana and Edward Salisbury Dana, Yale University, 1837–1892: halides, nitrates, borates, carbonates, sulfates, phosphates, arsenates, tungstates, molybdates. J. Wiley and Sons, New Jersey, USA.

Pasero, M. & Perchiazzi, N. (1996): Crystal structure refinement of matlockite. *Min. Mag.*, **60**, 833–836.

Pawley, G.S. (1981): Unit cell refinement from powder diffraction scans. *J. Appl. Crystallogr.*, **14**, 357–361.

Perchiazzi, N., Hålenius, U., Vignola, P., Demitri, N. (2018): Gabrielsonite revisited: crystal-structure determination and redefinition of chemical formula. *Eur. J. Mineral.*, **30**, 1173–1180.

Pertlik, F. (1978): The crystal structure of trigonite, $Pb_3Mn(AsO_3)_2(AsO_2\ OH)$. *Tscher. Min. Petrogr. Mitt.*, **25**, 95–105.

— (1987): The structure of freedite, $Pb_8Cu(AsO_3)_2O_3Cl_5$. *Mineral. Petrol.*, **36**, 85–92.

Sheldrick, G.M. (2013): SHELXS-2013 program for the crystal structure solution. University Göttingen, Göttingen, Germany.

Siidra, O.I., Krivovichev, S.V., Depmeier, W. (2007): Crystal chemistry of natural and synthetic lead oxohalides: II. Crystal structure of $Pb_7O_4(OH)_4Br_2$. *Proc. Russ. Mineral. Soc.*, **136**, 85–91.

Siidra, O.I., Krivovichev, S.V., Filatov, S.K. (2008a): Minerals and synthetic Pb(II) compounds with oxocentered tetrahedra: review and classification. *Z. Krist.*, **223**, 114–125.

Siidra, O.I., Krivovichev, S.V., Turner, R.W., Rumsey, M.S. (2008b): Chloroxiphite $Pb_3CuO_2(OH)_2Cl_2$: structure refinement and description in terms of oxocentred OPb_4 tetrahedra. *Mineral. Mag.*, **72**, 793–798.

—, —, —, — (2011): Natural and synthetic layered Pb(II) oxyhalides. in "Minerals as advanced materials II". Springer, Berlin, Heidelberg, 319–332.

Siidra, O.I., Krivovichev, S.V., Turner, R.W., Rumsey, M.S., Spratt, J. (2013a): Crystal chemistry of layered Pb oxychloride minerals with PbO-related structures: Part I. Crystal structure of hereroite,$[Pb_{32}O_{20}(O,\square)](AsO_4)_2[(Si, As, V, Mo)O_4]_2Cl_{10}$. *Am. Mineral.*, **98**, 248–255.

—, —, —, —, — (2013b): Crystal chemistry of layered Pb oxychloride minerals with PbO-related structures: Part II. Crystal structure of vladkrivovichevite, $[Pb_{32}O_{18}][Pb_4Mn_2O]Cl_{14}(BO_3)_8{\cdot}2H_2O$. *Am. Mineral.*, **98**, 256–261.

Siidra, O.I., Zinyakhina, D.O., Zadoya, A.I., Krivovichev, S.V., Turner, R.W. (2013c): Synthesis and modular structural architectures of mineralogically inspired novel complex Pb oxyhalides. *Inorg. Chem.*, **52**, 12799–12805.

Siidra, O.I., Kabbour, H., Mentré, O., Nazarchuk, E.V., Kegler, P., Zinyakhina, D.O., Colmont, M., Depmeier, W. (2016): Lead oxychloride borates obtained under extreme conditions. *Inorg. Chem.*, **55**, 9077–9084.

Sillén, L.G. & Melander, L. (1941): X-ray studies on the oxihalide minerals nadorite (ochrolite) $PbSbO_2Cl$ and ekdemite. *Z. Krist.*, **103**, 420–430.

Turner, R.W., Siidra, O.I., Krivovichev, S.V., Stanley, C.J., Spratt, J. (2012): Rumseyite, $[Pb_2OF]Cl$, the first naturally occurring fluoroxychloride mineral with the parent crystal structure for layered lead oxychlorides. *Mineral. Mag.*, **76**, 1247–1255.

Welch, M.D. (2004): Pb-Si ordering in sheet-oxychloride minerals: the super-structure of asisite, nominally $Pb_7SiO_8Cl_2$. *Mineral. Mag.*, **68**, 247–254.

Welch, M.D., Cooper, M.A., Hawthorne, F.C., Criddle, A.J. (2000): Symesite, $Pb_{10}(SO_4)O_7\ Cl_4(H_2O)$, a new PbO-related sheet mineral: Description and crystal structure. *Am. Mineral.*, **85**, 1526–1533.

Welin, E. (1968): Notes on the mineralogy of Sweden. 6. X-ray powder data for minerals from Långban and the related mineral deposits of central Sweden. *Arkiv Miner. Geol.*, **4**, 499–541.

Wilson, A.J.C. (1992): International Tables for Crystallography. Vol. **C**. Kluwer, Dordrecht, The Netherlands.

Received 5 November 2018
Modified version received 19 March 2019
Accepted 21 March 2019